A Region Merging Prior for Variational Level Set Image Segmentation

Ismail Ben Ayed, *Member, IEEE*, and Amar Mitiche, *Member, IEEE*

***Abstract*—In current level set image segmentation methods, the number of regions is assumed to known beforehand. As a result, it remains constant during the optimization of the objective functional. How to allow it to vary is an important question which has been generally avoided. This study investigates a *region merging prior* related to regions area to allow the number of regions to vary automatically during curve evolution, thereby optimizing the objective functional implicitly with respect to the number of regions. We give a statistical interpretation to the coefficient of this prior to balance its effect systematically against the other functional terms. We demonstrate the validity and efficiency of the method by testing on real images of intensity, color, and motion.**

***Index Terms*—Active contours, image segmentation, level sets, segmentation prior.**

I. Introduction

IMAGE segmentation occurs as a fundamental early vision processing task in many important applications. It consists of partitioning an image into regions which are homogeneous according to some description. Variational level set segmentation methods, which use active curves to delineate the segmentation regions, have been generally effective. The curve evolution equations are derived in a principled, flexible, and transparent way, from the minimization of a global objective functional. The level set representation of active curves [27] yields numerically stable and efficient algorithms. Several studies have shown that the variational, level set formalism can lead to effective segmentation algorithms [1], [4]–[6], [9], [10], [12], [17]–[19], [21], as well as effective algorithms to solve other vision problems such as tracking [13], motion estimation [14], and 3-D interpretation [15].

Although the actual number of segmentation regions is not known in most applications, current level set methods assume that it is given beforehand. It occurs as a constant in the objective functional and its optimization [1], [3], [6], [9], [10], [16]–[19], [21]. A few studies have considered determining the number of regions automatically, albeit as a process external to curve evolution. For instance, Brox and Weickert [23] estimate the number of regions in a preliminary stage by applying hierarchical level set splitting. The final segmentation is obtained by a classical functional minimization with a fixed number of regions. Zhu and Yuille [8] and Kadir and Brady [22] proposed to alternate local region merging[1] and curve evolution with a fixed number of regions. These methods are computationally costly and subject to the well known limitations of local region splitting/merging operations: (a) the results depend on several *ad hoc* parameters [22], [28], [29], such as thresholds to merge neighboring regions and the scale of local operations; (b) the results depend on the order of local operations [22], [28]; (c) local neighborhood search operations require additional costly definitions [8], [22]; (d) local region merging is sensitive to initial conditions [22].

The purpose of our study is to investigate a variational method which allows the effective number of regions to vary automatically during curve evolution. This is done via a *region merging prior* related to the regions area. This prior promotes region merging so that the objective functional is optimized *implicitly* with respect to the effective number of regions. A maximum number of regions, which is available in most applications, is used as a constant in the definition of the segmentation functional. Under the effect of the proposed region merging prior, the effective number of regions, equal to the maximum number of regions initially, decreases automatically during curve evolution to be, ideally, the desired number of regions.

A coefficient must be affected to the region merging prior in order to balance its contribution with respect to the other functional terms. This coefficient will, of course, affect the number of regions obtained. We will show that we can determine systematically an interval of values of this coefficient to obtain the desired number of regions. This is possible via a statistical interpretation of the coefficient over a set of relevant images and segmentation examples.

The region merging prior is used in conjunction with a data term which measures conformity to a piecewise constant segmentation model [4]–[6] and a length related term for smooth region boundaries.

To prevent the curves from intersecting, we use the partition constrained minimization scheme we proposed in [19], [20]. This scheme has a computational advantage over other methods [6], [10], [11], [16], [17]. It embeds an efficient partition constraint directly in the level set equations: if a point leaves a region, it goes to a single other region. Thus, starting from an arbi-

Manuscript received October 16, 2007; revised July 28, 2008. Current version published November 12, 2008. This work was supported by the Natural Sciences and Engineering Research Council of Canada under strategic Grant OGP0004234. The associate editor coordinating the review of this manuscript and approving it for publication was Dr. Mario A. T. (G. E.) Figueiredo.

I. Ben Ayed is with the Institut National de la Recherche Scientifique (INRS-EMT), Montréal, QC, H5A 1K6, Canada, and also with General Electric (GE) Canada, London, ON, N6A 4V2, Canada (e-mail: ismail.benayed@ge.com).

A. Mitiche is with the Institut National de la Recherche Scientifique (INRS-EMT), Montréal, QC, H5A 1K6, Canada (e-mail: mitiche@emt.inrs.ca).

Color versions of one or more of the figures in this paper are available online at http://ieeexplore.ieee.org.

Digital Object Identifier 10.1109/TIP.2008.2006425

[1]Region merging techniques rest on the repeated application of a statistical test to merge neighboring regions [28], [29].

trary initial partition with multiple curves, this constraint leads to a partition.

The remainder of this paper is organized as follows: After a presentation of segmentation into a fixed number of regions (Section II), we define (Section III) a general condition which a region merging prior must satisfy and propose a prior related to regions logarithmic area. We derive in Section IV the level set equations corresponding to the minimization of the objective functional. An interpretation of these equations will show the link between region merging and multiregion level set evolution: the proposed prior can cause some curves to disappear while other curves expand, thereby leading to a region merging by curve evolution, although not in the sense of the traditional one-step merging of two regions. We also give a statistical interpretation of the region merging prior coefficient. Section V describes validation experiments with real images of intensity, color, and motion.

II. Segmentation Into a Fixed Number of Regions

Segmenting an image $I : \Omega \subset \mathbb{R}^2 \rightarrow \mathbb{R}$ into N regions [1], [3], [9], [10], [16]–[19], [21] consists of determining a partition $\mathcal{R} = \{\mathbf{R}_k\}_{k\in[1,N]}$ of the image domain such that the image is homogeneous with respect to some characteristics in each region. Variational, level set segmentation is commonly stated as the minimization of a functional balancing the effect of two characteristic terms: a data term which measures the conformity of the image data within each region to a parametric model and a regularization term for smooth segmentation boundaries. Consider a partition $\mathcal{R} = \{\mathbf{R}_k\}_{k\in[1,N]}$ of Ω defined by a family of simple, closed plane curves $\vec{\gamma}_k|_{k=1,\ldots,N-1}$. For each k, region $\mathbf{R}_k$ corresponds to the interior $\mathbf{R}_{\vec{\gamma}_k}$ of curve $\vec{\gamma}_k$: $\mathbf{R}_k = \mathbf{R}_{\vec{\gamma}_k}$. Let region $\mathbf{R}_N$ be the intersection of the exteriors of all curves: $\mathbf{R}_N = \bigcap_{k=1}^{N-1} \mathbf{R}_k^c$. Using the piecewise constant model[2] [4], [6] and a regularization term related to the length of region boundaries [7], multiregion active curve segmentation consists of determining $\vec{\gamma}_k|_{k=1,\ldots,N-1}$ that minimize the following functional:

$$\mathcal{F}\left(\{\vec{\gamma}_k\}_{k=1}^{N-1}\right) = \sum_{k=1}^{N} \int_{\mathbf{R}_k} \|I-\mu_k\|^2 + \lambda \sum_{k=1}^{N-1} \oint_{\vec{\gamma}_k} ds \quad (1)$$

where μ_k is a parameter of region $\mathbf{R}_k$ ($k \in [1,\ldots,N]$), and λ is a positive real constant to weigh the relative contribution of the two terms of the functional. Optimization of functional $\mathcal{F}$ with respect to the region parameters determines these as the intensity mean values inside regions [4], [6]

$$\mu_k = \frac{\int_{\mathbf{R}_k} I(\mathbf{x})d\mathbf{x}}{\int_{\mathbf{R}_k} d\mathbf{x}}. \quad (2)$$

Optimization of functional $\mathcal{F}$ with respect to $\vec{\gamma}_k|_{k=1,\ldots,N-1}$ yields the curve evolution equations [6].

The simple example in Fig. 1 illustrates the usefulness of adding a region merging term to this type of functional. Consider an image composed of two non intersecting regions, $\mathbf{R}_1$ and $\mathbf{R}_2$, and a background region $\mathbf{R}_3 = (\mathbf{R}_1 \cup \mathbf{R}_2)^c$. Let the intensities in $\mathbf{R}_1$, $\mathbf{R}_2$, and $\mathbf{R}_3$ be constant and equal, respectively, to μ_1, μ_2, and μ_3. In the special case where $\mu_1 = \mu_2$, there is no incentive in model (1) to merge $\mathbf{R}_1$ and $\mathbf{R}_2$ because $\sum_{k=1}^{3} \int_{\mathbf{R}_k} \|I-\mu_k\|^2 = 0$ corresponds to the minimum of the data term. More generally, one can show for two non intersecting regions, $\mathbf{R}_1$ and $\mathbf{R}_2$, that [26]

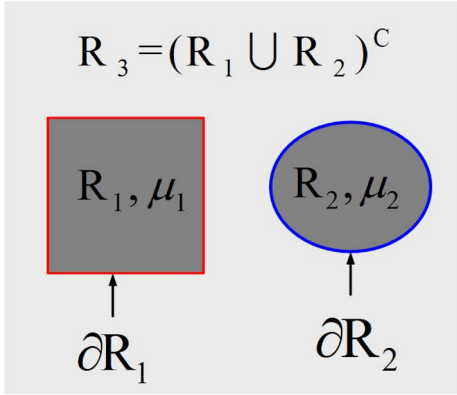

Fig. 1. Minimization of functional (1) with $N = 3$ may lead to a segmentation into three regions of an image containing uniquely two regions.

$$\int_{\mathbf{R}_1} \|I-\mu_1\|^2 + \int_{\mathbf{R}_2} \|I-\mu_2\|^2 \leq \int_{\mathbf{R}_1\cup\mathbf{R}_2} \|I-\mu_{1,2}\|^2$$
$$\lambda(\partial\mathbf{R}_1 + \partial\mathbf{R}_2) = \lambda\partial(\mathbf{R}_1 \cup \mathbf{R}_2)$$

where μ_1, μ_2, and $\mu_{1,2}$ are the mean of $\mathbf{R}_1$, $\mathbf{R}_2$, and $\mathbf{R}_1 \cup \mathbf{R}_2$, respectively. The minimization of (1) does not favor merging $\mathbf{R}_1$ and $\mathbf{R}_2$, *even when* $\mu_1 = \mu_2$. As we will show in several experiments (Section V), model (1) may lead to an over-segmentation when N is larger than the actual number of regions. An additional term in (1) which can merge regions, as when $\mu_1 = \mu_2$, would be beneficial. In this study, we propose and investigate such a term.

III. Region Merging Prior

A region merging prior $\mathcal{P}_{\mathcal{RM}}$ is a function which maps the set of partitions of Ω to $\mathbb{R}$. It must satisfy the following condition:

For each partition $\mathcal{R} = \{\mathbf{R}_k\}_{k=1}^{N}$ *of* Ω, *and for each subset* $\mathcal{J}$ *of* $[1\ldots N]$

$$\mathcal{P}_{\mathcal{RM}}\left(\left\{\cup_{j\in\mathcal{J}}\mathbf{R}_j, \{\mathbf{R}_k\}_{k\in[1\ldots N],k\notin\mathcal{J}}\right\}\right) < \mathcal{P}_{\mathcal{RM}}\left(\{\mathbf{R}_k\}_{k=1}^{N}\right). \quad (3)$$

This condition means that any region merging must decrease the prior term. We propose the following prior[3] which satisfies the region merging condition (3):

$$\mathcal{P}_{\mathcal{RM}}\left(\{\mathbf{R}_k\}_{k=1}^{N}\right) = -\beta \sum_{k=1}^{N} a_k \log a_k \quad (4)$$

where a_k is the area of region $\mathbf{R}_k$, i.e.,

$$a_k = \int_{\mathbf{R}_k} d\mathbf{x} \quad (5)$$

and β is a positive real constant to weigh the relative contribution of the region merging term in the segmentation functional.

[2]We use this model to simplify the presentation. We may, however, use other models [9], [18].

[3]For $a_k = 0$, we pose $a_k \log a_k = 0$.

The proposed region merging prior has an entropic interpretation. If we define the probability of a region $\mathbf{R}_k$ by $p_k = a_k/A$, where A is the area of Ω, we have

$$-\beta \sum_{k=1}^{N} a_k \log a_k = -\beta.A. \sum_{k=1}^{N} \frac{a_k}{A} log \frac{a_k}{A} - \beta.A. \log A$$
$$= \beta.A.H\left(\{\mathbf{R}_k\}_{k=1}^{N}\right) - \beta.A. \log A$$

where H is the partition entropy. $-\beta.A.\log A$ is a constant independent from the partition and can be ignored. As we will see in Section IV-C, the logarithmic form of this prior has an interesting property which leads to a statistical interpretation that allows fixing the weight of the region merging term systematically.

It is worth noting that a region-competition prior with a minimum description length (MDL) interpretation has been proposed in [8], and used in [22] and [23], to merge segmentation regions. The prior is expressed as a constant multiplied by the number of regions

$$\mathcal{P}_{\text{region-competition}} = \nu N. \tag{6}$$

As shown subsequently, the region merging prior in this study has several advantages over the region-competition prior. First, it allows region merging to occur during curve evolution (Section IV-B). By contrast, the prior in [8] is independent of the curves and, therefore, does not affect curve evolution. As a result, local region-merging operations are added to alter the number of regions [8], [22]. Second, there is no clear indication on how to fix the weight of the region-competition prior, by contrast to the region merging prior (Section IV-C). Third, the computational load is significantly less using the region merging prior because the solution is reached after one stage of curve evolution whereas several stages are required with the region-competition prior, each stage consisting of curve evolution followed by local region-merging operations (Section V). Finally, it leads to a segmentation method which is more robust with respect to the initial number of regions (Section V).

IV. Segmentation Functional

Let N be the maximum number of regions, i.e., a number such that the actual number of regions is inferior or equal to N. Such a number is available in most applications. With the region merging prior (4), the functional of segmentation into a number of regions less than N is

$$\mathcal{F}_{\mathcal{RM}}\left(\{\vec{\gamma}_k\}_{k=1}^{N-1}\right) = \underbrace{\sum_{k=1}^{N} \int_{\mathbf{R}_k} \|I - \mu_k\|^2}_{\text{Data term}} \underbrace{-\beta \sum_{k=1}^{N} a_k \log a_k}_{\text{Region merging prior}} + \underbrace{\lambda \sum_{k=1}^{N-1} \oint_{\vec{\gamma}_k} ds}_{\text{regularization}}. \tag{7}$$

In the following sections, we will derive the level set evolution equations corresponding to (7) (Section IV-A) and then show how the effective number of active curves can decrease automatically as a result of the region merging prior (Section IV-B).

A. Level Set Equations

We minimize $\mathcal{F}_{\mathcal{RM}}$ with respect to the curves $\vec{\gamma}_k$, $k = 1, \ldots, N-1$, by embedding these into a family of one-parameter curves $\vec{\gamma}_k(s,t) : [0,1] \times \mathbb{R}^+ \rightarrow \Omega$ and solving the partial differential equations

$$\frac{d\vec{\gamma}_k}{dt} = -\frac{\partial \mathcal{F}_{\mathcal{RM}}}{\partial \vec{\gamma}_k}, \quad k = 1, \ldots, N-1. \tag{8}$$

Multiregion segmentation uses several active curves. When the interior of each curve defines a region, curve evolution equations must not lead to overlapping regions so that these define a partition of the image domain. Several methods have been devised for curve evolution to lead to a partition [6], [10], [11], [16], [17], [20]. Here, we use the partition constrained minimization scheme we developed in [19], [20]. This scheme has advantages over others because it is fast, stepwise optimal, i.e., results in a maximum decrease of the functional at each evolution iteration, and is robust to initialization [19], [20]. It embeds an efficient partition constraint directly in the level set evolution equations: if a point leaves a region $\mathbf{R}_i$, it goes to a single other region $\mathbf{R}_j$. Starting from an arbitrary initial partition, this simple constraint leads to a partition [19], [20]. At each iteration, the scheme involves only two regions for each pixel $\mathbf{x}$, a region $\mathbf{R}_i$ which contains $\mathbf{x}$ currently, and a region $\mathbf{R}_j$, $j \neq i$, which corresponds to the largest decrease in the functional were $\mathbf{x}$ transferred to this region (refer to [19] and [20] for details).

For a level set implementation[4] of curve evolution equations $\partial\vec{\gamma}_k/\partial t$, $k = 1, \ldots, N$, we represent each curve $\vec{\gamma}_k$ implicitly by the zero level set of a function $u_k : \mathbb{R}^2 \rightarrow \mathbb{R}$, with the region inside $\vec{\gamma}_k$ corresponding to $u_k > 0$. To compute the partition constrained level set equations minimizing (7), we use our result in [20] which shows that for a segmentation functional $\mathcal{F}$ having the form

$$\mathcal{F}\left(\{\vec{\gamma}_k\}_{k=1}^{N-1}\right) = \sum_{k=1}^{N} \int_{\mathbf{R}_k} e_k(\mathbf{x}) d\mathbf{x} + \lambda \sum_{k=1}^{N-1} \oint_{\vec{\gamma}_k} ds \tag{9}$$

with e_k, $k = 1, \ldots, N$, scalar functions, the multiregion partition constrained level set equations minimizing $\mathcal{F}$ are given, at each $\mathbf{x} \in \Omega$, by

$$\text{if } i \neq N, \ \frac{\partial u_i}{\partial t}(\mathbf{x},t) = -\left(e_i(\mathbf{x}) - e_j(\mathbf{x}) + \lambda\kappa_{u_i}\right) \times \left\|\vec{\nabla} u_i(\mathbf{x},t)\right\|$$
$$\text{if } j \neq N, \ \frac{\partial u_j}{\partial t}(\mathbf{x},t) = -\left(e_j(\mathbf{x}) - e_i(\mathbf{x}) + \lambda\kappa_{u_j}\right) \times \left\|\vec{\nabla} u_j(\mathbf{x},t)\right\| \tag{10}$$

where κ_{u_k} is the curvature of the zero level-set of u_k, $i \in [1 \ldots N]$ is the index of the region containing $\mathbf{x}$, and j is given by

$$j = \arg \min_{\{k \in [1 \ldots N], \mathbf{x} \notin \mathbf{R}_k\}} e_k(\mathbf{x}). \tag{11}$$

[4]The level set implementation handles automatically topological changes of the evolving curve and yields an implicit, numerically stable representation of the corresponding region membership and boundary which removes the need of complex data structures [27].

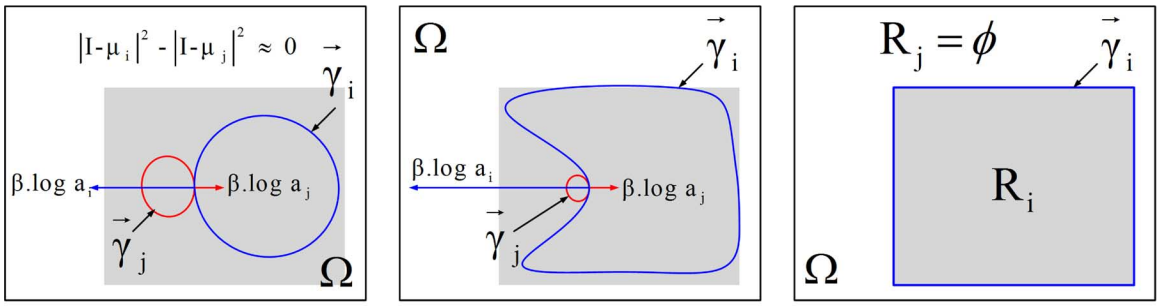

Fig. 2. Region merging interpretation of the curve evolution equations. (a), (b) Evolution of two homogeneous active regions under the effect of the region merging prior velocity: $a_i > a_j$ results in expanding $\mathbf{R}_i$ and shrinking $\mathbf{R}_j$; (c) only one curve $(\vec{\gamma}_i)$ encloses both regions while the other curve, $\vec{\gamma}_j$, disappears.

Note that the studies in [23] and [24] used similar equations for coupling level set evolution. The difference here is that the partition constrained scheme (10) activates at most two level set equations at each iteration.

To use result (10) here, we rewrite functional $\mathcal{F}_{\mathcal{RM}}$ (7) as follows (we replace $a_k \log a_k$ by $\int_{\mathbf{R}_k} \log a_k$):

$$\begin{aligned}\mathcal{F}_{\mathcal{RM}}\left(\{\vec{\gamma}_k\}_{k=1}^{N-1}\right) &= \sum_{k=1}^{N} \int_{\mathbf{R}_k} \|I-\mu_k\|^2 - \beta \sum_{k=1}^{N} \int_{\mathbf{R}_k} \log a_k \\ &\quad + \lambda \sum_{k=1}^{N-1} \oint_{\vec{\gamma}_k} ds \\ &= \sum_{k=1}^{N} \int_{\mathbf{R}_k} \underbrace{\left(\|I-\mu_k\|^2 - \beta \log a_k\right)}_{e_k} \\ &\quad + \lambda \sum_{k=1}^{N-1} \oint_{\vec{\gamma}_k} ds. \end{aligned} \tag{12}$$

Thus, applying the results (10) and (11) to $e_k = \|I-\mu_k\|^2 - \beta \log a_k$ yields, at each $\mathbf{x} \in \Omega$, the partition constrained level set evolution equations minimizing $\mathcal{F}_{\mathcal{RM}}$

$$\begin{aligned}\text{if } i \neq N,\ \frac{\partial u_i(\mathbf{x},t)}{\partial t} &= -\Bigg(\underbrace{\|I(\mathbf{x})-\mu_i\|^2 - \|I(\mathbf{x})-\mu_j\|^2}_{\text{Region competition}} \\ &\qquad - \underbrace{\beta(\log a_i - \log a_j)}_{\text{Region merging}} + \lambda \kappa_{u_i} \Bigg) \\ &\quad \times \left\| \vec{\nabla} u_i(\mathbf{x},t) \right\| \\ \text{if } j \neq N, \frac{\partial u_j(\mathbf{x},t)}{\partial t} &= -\Big(\|I(\mathbf{x})-\mu_j\|^2 - \|I(\mathbf{x})-\mu_i\|^2 \\ &\qquad - \beta(\log a_j - \log a_i) + \lambda \kappa_{u_j} \Big) \\ &\quad \times \left\| \vec{\nabla} u_j(\mathbf{x},t) \right\| \end{aligned} \tag{13}$$

where $i \in [1 \ldots N]$ is the index of the region containing $\mathbf{x}$, and j is given by

$$j = \arg \min_{\{k \in [1 \ldots N], \mathbf{x} \notin \mathbf{R}_k\}} \|I-\mu_k\|^2 - \beta \log a_k. \tag{14}$$

B. Region Merging Interpretation of the Level Set Evolution Equations

The level set equations (13) show how region merging occurs intrinsically in multiple curve evolution. When two disjoint regions $\mathbf{R}_{\vec{\gamma}_i}$ and $\mathbf{R}_{\vec{\gamma}_j}$ have close intensities [Fig. 2(a)], the velocity resulting from the data term is weak ($\|I-\mu_j\|^2 - \|I-\mu_i\|^2 \approx 0$). Ignoring the curvature term, evolution of curves $\vec{\gamma}_i$ and $\vec{\gamma}_j$ is guided principally by the region merging prior velocity. As u_i increases and u_j decreases under the effect of $(\log a_i - \log a_j)$, this velocity expands the region having the larger area [Fig. 2(b)], and shrinks the other region, and this until only one curve encloses both regions and the other curve disappears [Fig. 2(c)].

C. How to Fix the Weighting Parameter β

On one hand, the data term increases when regions are merged. On the other hand, the region merging term, $-\sum_{k=1}^{N} a_k \log a_k$, decreases when regions are merged. The role of the weighting parameter β is to balance the contribution of the region merging term against the other terms so as to, ideally, correspond to the actual number of regions.

Note that the weighting parameter β can be viewed as a *unit conversion factor* between the units of the data and the region merging terms. Therefore, and considering the form of these terms, we can take[5]

$$\beta = \alpha \frac{\int_\Omega \|I-\mu\|^2}{A.\log A} \quad \forall A > 1 \tag{15}$$

where μ is the mean intensity over the whole image, A is the image domain area, and α is a constant without unit. Note that $\int_\Omega \|I-\mu\|^2 / A.\log A$ is independent of the segmentation and is the ratio of the data term to the region merging term in the case of a partition with a single region (which corresponds to the whole

[5]Formally, we have: $A = \int_\Omega d\mathbf{x}$. In practice, A is an integer corresponding to the number of pixels in the image. Consequently, we ignore the cases $A = 0$ and $A = 1$.

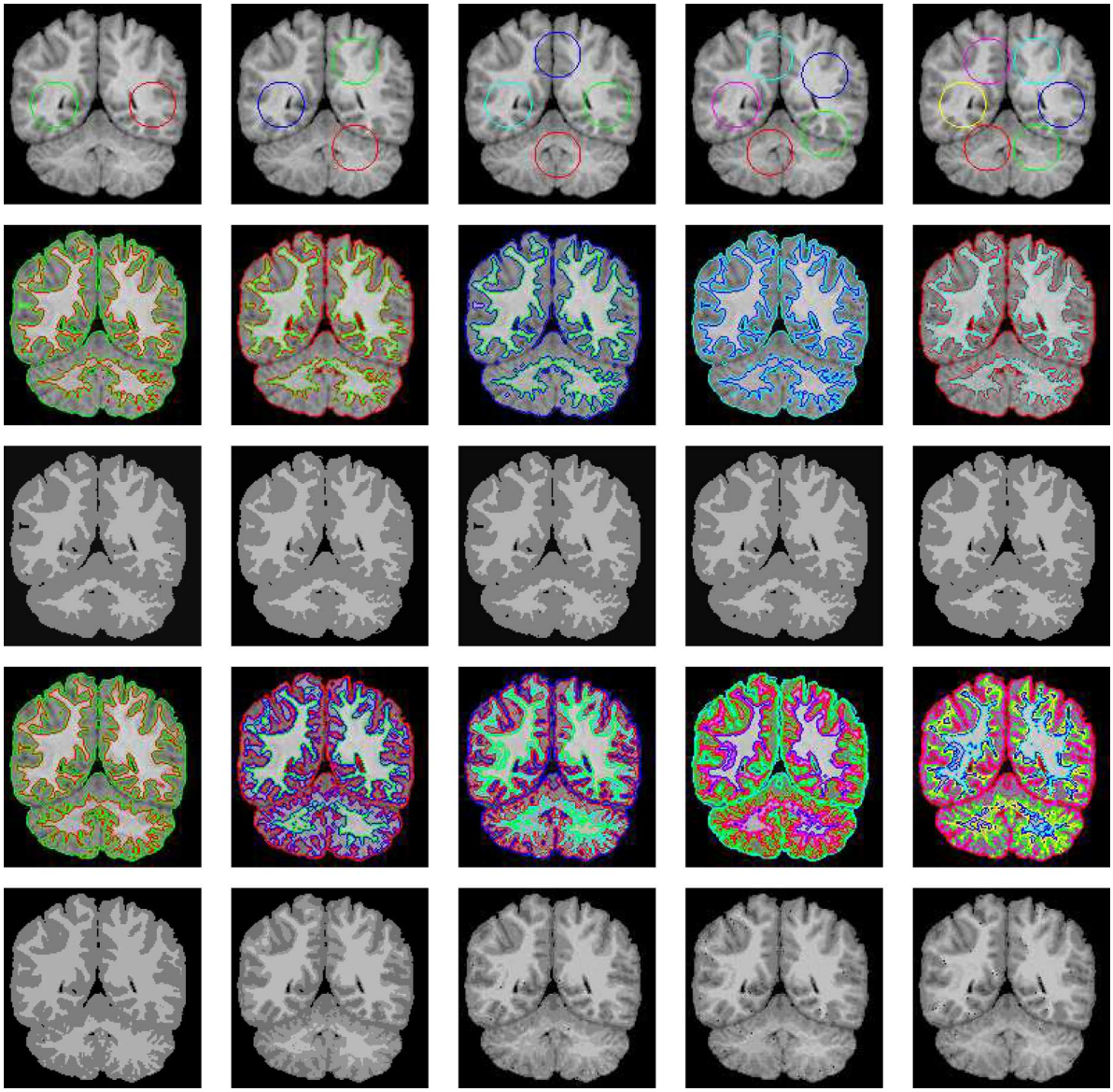

Fig. 3. Segmentation of a brain image. Line 1: Different number of regions at the initialization; line 2: final curves which remained at convergence *with* the region merging prior ($\alpha = 1$); line 3: final segmentations *with* the region merging prior $\alpha = 1$); line 4: final curves (N curves) *without* the region merging prior ($\alpha = 0$); line 5: final segmentations *without* the region merging prior ($\alpha = 0$). The displayed results are obtained with $\lambda = 2$.

image domain). Using expression (15), we rewrite the sum of the data term and the region merging prior as follows:

$$\sum_{k=1}^{N} \int_{\mathbf{R}_k} ||I - \mu_k||^2 - \alpha \underbrace{\frac{\sum_{k=1}^{N} a_k \log a_k}{A.\log A}}_{\text{close to 1}} \int_{\Omega} ||I - \mu||^2. \quad (16)$$

Note that the denominator in (15) can be viewed as a normalizing factor for the prior and the integral in the numerator as a normalizing factor for the data term because minimizing (16) is equivalent to minimizing

$$\underbrace{\frac{\sum_{k=1}^{N} \int_{\mathbf{R}_k} ||I - \mu_k||^2}{\int_{\Omega} ||I - \mu||^2}}_{\in [0,1]} - \alpha \underbrace{\frac{\sum_{k=1}^{N} a_k \log a_k}{A.\log A}}_{\in [0,1]}. \quad (17)$$

Therefore, a value of α close to 1 would seem reasonable. The following analysis and the experiments in Section V show that this is the case.

We note the following important inequalities for any partition $\mathcal{R} = \{\mathbf{R}_k\}_{k=1}^{N}$ of Ω

$$1 - \frac{\log N}{\log A} \leq \frac{\sum_{k=1}^{N} a_k \log a_k}{A.\log A} \leq 1 \quad \forall A > 1. \quad (18)$$

Proof: The right hand inequality in (18), $(\sum_{k=1}^{N} a_k \log a_k / A.\log A) \leq 1$, is a straightforward application of condition (3). For the left-hand inequality, applying

$$\log(z) \leq z - 1, \forall z \in [0, +\infty[$$

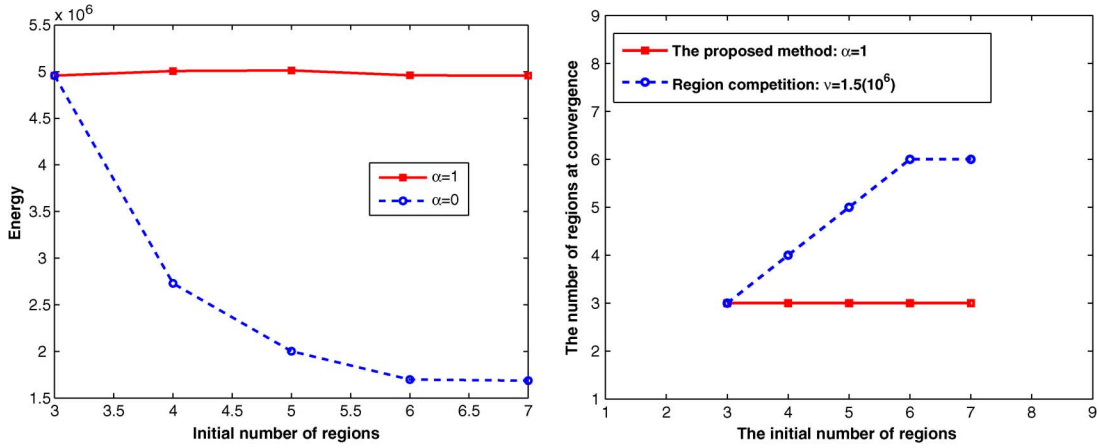

(a) (b)

Fig. 4. (a) Effect of the region merging prior: graph of the minimized data term versus the initial (maximum) number of regions (N). (b) The number of regions obtained at convergence versus the initial number of regions for the region-competition algorithm [8], [22] and the proposed method.

TABLE I
BRAIN IMAGE: EFFECT OF PARAMETER α ON THE NUMBER OF REGIONS

α	$2.31 \leq \alpha \leq 7.10$	$0.58 \leq \alpha \leq 2.29$	$0.36 \leq \alpha \leq 0.56$
regions	2	3	4

TABLE II
BRAIN IMAGE: EFFECT OF PARAMETER ν ON THE NUMBER OF REGIONS AT CONVERGENCE FOR THE REGION-COMPETITION ALGORITHM [8], [22]. 3-REGION INITIALIZATION: ν VALUES STOPPING THE REGION MERGING. 4-REGION TO 7-REGION INITIALIZATIONS: ν VALUES ALLOWING THE REGION MERGING

Initial number of regions	7	6	5	4	3
ν (Region competition)	$[0.93(10^6), +\infty[$	$[(1.87(10^6), +\infty[$	$[2.73(10^6), +\infty[$	$[(2.43(10^6), +\infty[$	$[0, 1.55(10^6)[$

TABLE III
COMPUTATION TIME FOR THE SEGMENTATION OF THE BRAIN IMAGE WITH DIFFERENT INITIALIZATIONS: THE INITIAL NUMBER OF REGIONS VARIES FROM 3 TO 7

Initial number of regions	3	4	5	6	7
The proposed method	0.22s	0.25s	0.3s	0.35s	0.4s
The region-competition algorithm ($\nu = 1.5(10^6)$) [8], [22]	0.65s	0.78s	1.04s	1.41s	3.21s

to $1/Np_k$, where $p_k = a_k/A, \forall k \in [1 \dots N]$, gives

$$\log\left(\frac{1}{Np_k}\right) \leq \frac{1}{Np_k} - 1, \ \forall k \in [1 \dots N]. \tag{19}$$

Multiplying by p_k both sides of (19) yields

$$\begin{aligned} p_k \log\left(\frac{1}{Np_k}\right) &\leq \frac{1}{N} - p_k, \ \forall k \in [1 \dots N] \\ \Rightarrow \sum_{k=1}^{N} p_k \log\left(\frac{1}{Np_k}\right) &\leq \underbrace{1 - \sum_{k=1}^{N} p_k}_{0} \\ \Rightarrow -\sum_{k=1}^{N} \frac{a_k}{A} \log\frac{a_k}{A} &\leq \log(N) \\ \Rightarrow \frac{\sum_{k=1}^{N} a_k \log a_k}{A.\log A} &\geq 1 - \frac{\log N}{\log A} \end{aligned}$$

which completes the proof of (18).

In practice, N is generally much smaller than A and $\sum_{k=1}^{N} a_k \log a_k / A.\log A$ is close to 1. For example, for a maximum number of regions equal to 10 and a 256×256 image, we have approximately $0.8 \leq (\sum_{i=1}^{N} a_i \log a_i)/A.\log A \leq 1$.

The small interval of variation of the normalized prior in (18) suggests that α will vary in a small interval centered close to 1. This will be confirmed experimentally. For several image classes, we will show that we can take α in an interval containing, or close to, 1, and which we can use for all the images of the same class. We will give examples with images of intensity, color, and motion. Note that with a value of α close to 1 in (16), the sum of the data and the region merging terms will be close to the in-between cluster distance in accor-

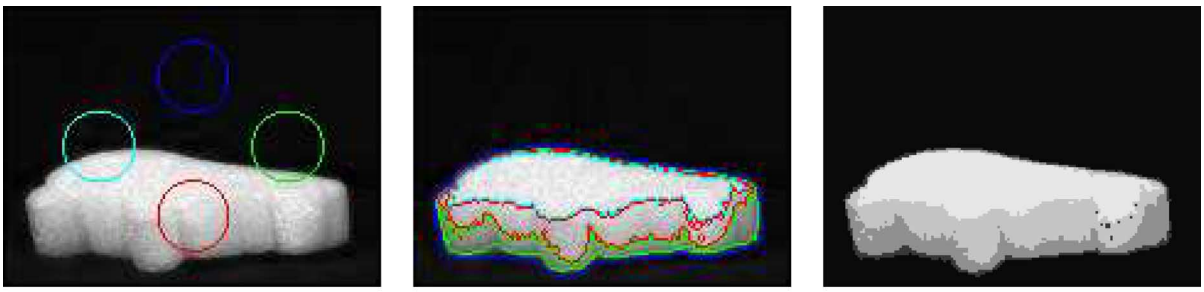

(a) (b) (c)

Fig. 5. Results without the region merging prior ($\alpha = 0$) on an image compound of two regions (object and background): (a) initialization ($N = 5$, i.e., 4 curves), (b) final curves, (c) final segmentation into five regions.

dance to the classical data clustering relation in statistical pattern recognition [26]

$$\underbrace{\sum_{k=1}^{N} \int_{\mathbf{R}_k} ||I - \mu_k||^2}_{\text{within-cluster distance}} - \underbrace{\int_{\Omega} ||I - \mu||^2}_{\text{total distance}} = \underbrace{-\sum_{k=1}^{N} ||\mu_k - \mu||^2}_{\text{in-between cluster distance}} . \quad (20)$$

D. How to Fix the Regularization Parameter λ

We can fix the value of the regularization parameter λ using the minimum description length (MDL) interpretation of this parameter as was done in [2]. This interpretation prescribes a value of parameter λ approximately equal to 2 [2]. It is interesting that experimental simulations in [2] show that this value corresponds to the minimum of the mean number of misclassified pixels.

V. Experiments

We conducted a large number of tests with different image types to demonstrate the effect of the region merging prior. The method has been also compared to the region-competition algorithm [8] in regard to the optimal number of regions and computational load. Here following is a representative sample of the results obtained using real images of intensity, color, and motion.

A. Gray Level Images

Influence of the Proposed Region Merging Prior: Fig. 3 shows segmentations of a brain image for different initial (maximum) number of regions (N vary from three to seven regions). The first line of Fig. 3 depicts the curve initializations corresponding to the different values of N. To illustrate the influence of the region merging prior, we show the results obtained *with* the region merging prior ($\alpha = 1$) in the second and third lines, and the results obtained *without* the region merging prior ($\alpha = 0$) in the fourth and fifth lines. *With* the region merging prior, some curves disappear at convergence (second line), leading to the same correct segmentation into three regions (third line) for N (the initial number of regions) going from 3 to 7 (first line). *Without* the region merging prior, none of the curves disappears and the functional minimization splits up the image into exactly N regions leading to five different segmentations (fifth line). In order to illustrate more clearly the effect of the region merging prior, we plotted in Fig. 4(a) the data term at convergence versus N, for $\alpha = 0$ and $\alpha = 1$ (without and with the region merging prior). For $\alpha = 0$ (discontinuous curve), the minimized data term decreases when N increases. The region merging prior, which increases with N, balances the effect of the data term, leading approximately to the same value of the functional at convergence for the different values of N (continuous curve). These experiments also show the robustness of the method with respect to the initial (maximum) number of regions.

TABLE IV
Color Images: Intervals of α Values Corresponding to the Desired Number of Regions

Color image	α_{min}	α_{max}
1	1.49	5.6
2	1.00	3.97
3	1.35	4.37
4	0.36	5.5
5	1.03	2.67
6	0.096	3.81

We also evaluated the effect of parameter α on the number of segmentation regions at convergence, using 7 initial regions ($N = 7$). Table I lists the number of regions obtained at convergence, and the interval of α values leading to this number. All the values of α in the interval [0.58, 2.29] give the same segmentation of the brain image into the desisred number of regions, i.e., three regions. This is consistent with the statistical interpretation we gave in Section IV-C of the weight of the region merging prior, and which led to a value of α of about 1. In later experiments with images of color and motion, we will

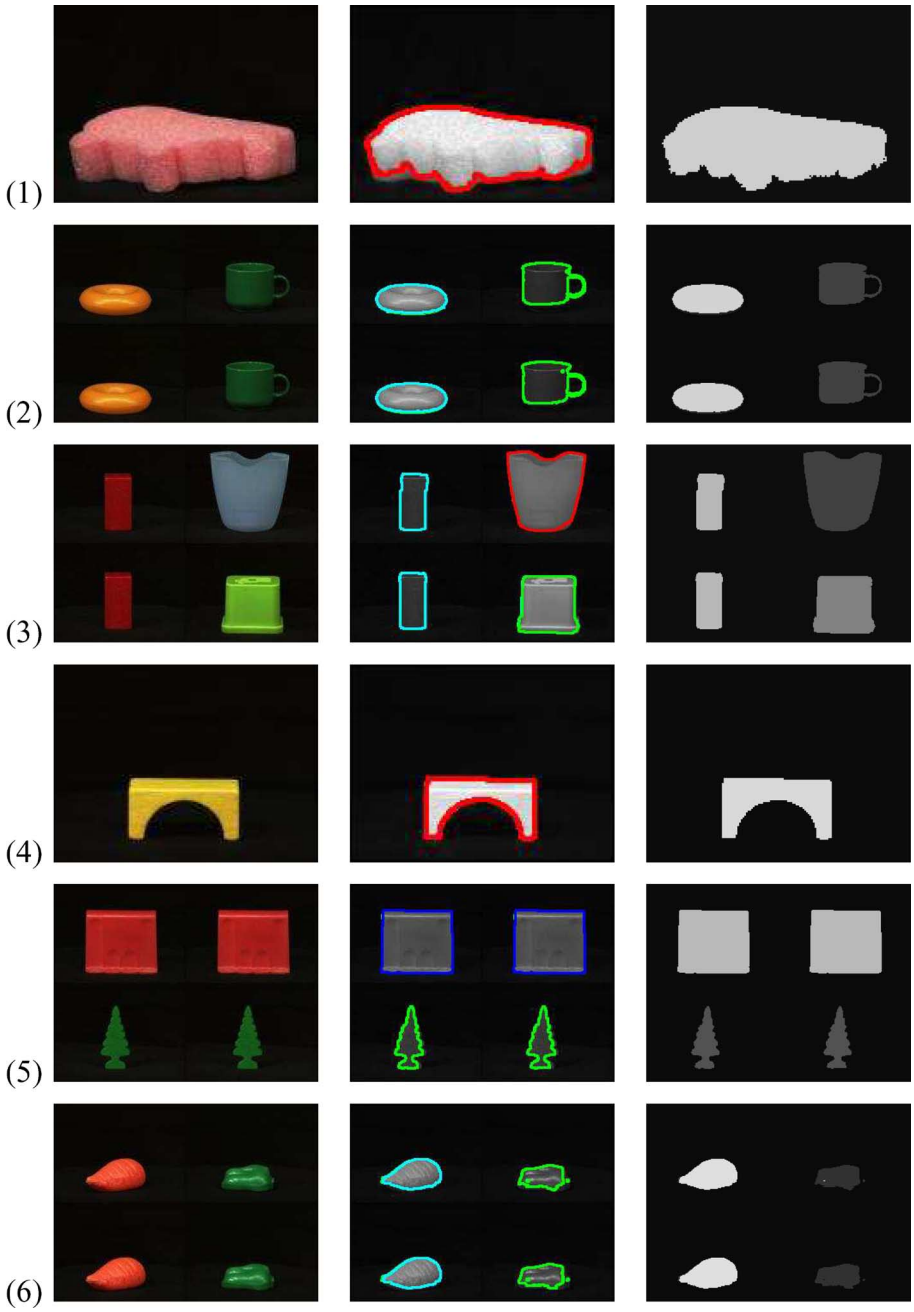

Fig. 6. Segmentation results using the region merging prior for 6 color images from the same database: images (1)–(6) (first column); final curves which remained at convergence (second column); final segmentations (third column). The displayed results are obtained with $\alpha = 2$ and $\lambda = 2$.

confirm that we can determine automatically, or by learning, an interval of α values applicable to the images of a given class.

Comparisons With the Region-Competition Algorithm [8], [22]: By contrast to the proposed method, the region-competition algorithm, which uses a prior expressed as a constant ν multiplied by the number of regions: $\mathcal{P}_{\text{region-competition}} = \nu N$, is sensitive to the initial number of regions. For instance, it cannot lead to the same segmentation of the brain image into three regions for the five different initializations in Fig. 3 (the initial number of regions varies from 3 to 7). Table II lists, for each initialization, the intervals of ν values necessary to obtain three regions at convergence with the region-competition algorithm. To stop the region merging with a 3-region initialization, i.e., to obtain segmentation into three regions, ν should be in $[0, 1.55(10^6)]$. However, all ν values in this interval do not allow region merging with 6-region, 5-region, and 4-region initializations (refer to Table II), thereby resulting in four different segmentations of the brain image. With the proposed region merging prior, all α values in [0.58, 2.29] give the same segmentation into three regions (refer to Table I). We plotted in Fig. 4(b) the number of regions obtained at convergence versus the initial number of regions for the region-competition algorithm and the proposed method. The proposed prior leads to a segmentation method which is more robust to the variations of the initial number of regions.

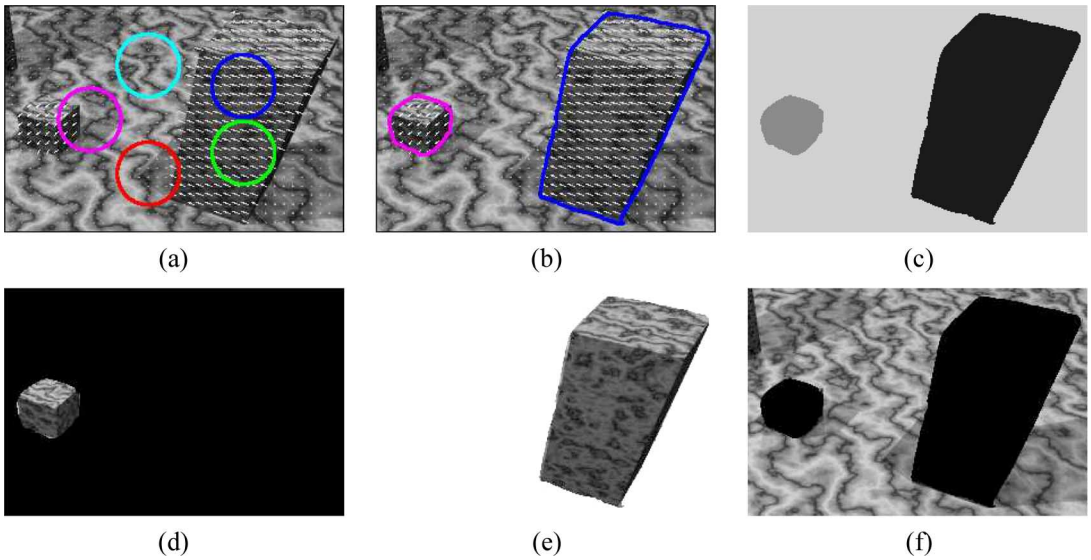

Fig. 7. Segmentation results with the Marmor sequence ($\alpha = 2$): (a) five initial curves (six regions) and the motion field (two moving objects); (b) two final curves corresponding to the moving objects; (c) obtained segmentation into three regions (two moving objects and a background); (d), (e) segmentation regions corresponding to moving objects; (f) segmentation region corresponding to the background.

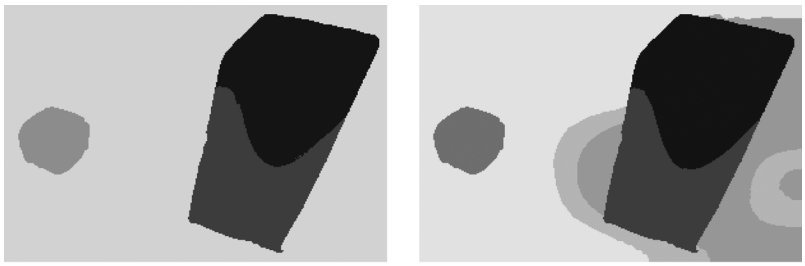

Fig. 8. Segmentation results without the region merging prior (Marmor sequence, $\alpha = 0$): (a) segmentation with $N = 4$; (b) segmentation with $N = 6$.

Table III reports the computation time on a 2-GHz machine for the proposed method and the region-competition algorithm. We used the brain image with different initializations: the initial number of regions varies from 3 to 7. The proposed method leads to a significant decrease in computation load, particularly when the initial number of regions augments. This is expected because the solution is reached after one stage of curve evolution whereas the region-competition algorithm alternates iteratively two stages: curve evolution and local region-merging operations.

B. Vector-Valued Image Segmentation

For a vector-valued image represented by L images, the data term in functional (7) can be generalized [5] as

$$\sum_{k=1}^{N} \int_{\mathbf{R}_k} \sum_{l=1}^{L} \left\| I^l - \mu_k^{(l)} \right\|^2 \tag{21}$$

where I^l ($l \in [1 \dots L]$) is image l and $\mu_k^{(l)}$ is the constant for image l in the segmentation region k. We show segmentation examples of color images in Section V-B1 and of motion in Section V-B2.

1) Color Images: The RGB space is used to represent the color information in each image. We show, here, results for a set of 6 images, each image containing several objects [Fig. 6, (1)–(6)]. The objects in these images were taken from ALOI database [25]. We have images with two, three and four regions. Segmentation of these images without fixing the number of regions is difficult due to the illumination variations inside each object. Fig. 5 gives the segmentation result, *without* the region merging prior, of the color image (1) shown in Fig. 6. This image consists of two regions: an object and a background. Segmentation of this image into five regions gives the final curves displayed in Fig. 5(b) and the segmentation shown in Fig. 5(c). The corresponding initialization with four curves is depicted in Fig. 5(a). *Without* the region merging prior, the object is fragmented into four different regions due to illumination variations. The first line in Fig. 6 shows the segmentation results of the same image in Fig. 5 *with* the region merging prior. Only one curve (red) remained at convergence. This final curve separates correctly the object from the background. With the same initialization (five regions, four curves) in Fig. 5(a), and using the same α ($\alpha = 2$), the other images [from (2) to (6)] have also been segmented correctly. The columns of Fig. 6 show, respectively, the image, the final curves remaining at convergence, and the corresponding final segmentation. The final segmentation of each image corresponds to desired number of regions as well as to the objects. We evaluated the interval of α values,

(a) (b) (c) (d)

Fig. 9. Segmentation results with the Road sequence: (a) five initial curves (6 regions) and the motion field (one moving object); (b) one final curve; (c) segmentation region corresponding to the moving object (inside the curve); (d) segmentation region corresponding to the background (outside the curve).

$[\alpha_{\min}, \alpha_{\max}]$, which lead to the desired number of regions for each image. The obtained intervals are reported in Table IV. All α values in [1.49, 2.67] lead to a correct segmentation of the six images. These results conform to expectations, and to the statistical interpretation we gave in Section IV-C to coefficient α.

2) Motion Segmentation: In this experiment, we segment optical flow images into motion regions. Optical flow at each pixel is a 2-D vector and segmentation is performed by minimizing a functional containing the data term (21), the region merging prior, and the length-related regularization term. We show two examples.

The first example uses the Marmor sequence, which contains three regions: two moving objects and a background. The method in [14] was used to estimate the optical flow. The initial curves (five curves for at most six regions) and motion vectors are shown in Fig. 7(a). *With* the region merging prior, Fig. 7(b) depicts curves which remained giving a correct segmentation into three regions [Fig. 7(c)]. In this example, $\alpha = 2$. Fig. 7(d) and (e) shows regions corresponding to the two moving objects, and (f) shows the background. To illustrate the effect of the region merging prior, Fig. 8(b) shows the segmentation obtained using the same initialization $(N = 6)$ but *without* the region merging prior $(\alpha = 0)$. The background, in this case, is divided into three different regions, and the moving object on the right is divided into two regions. We also give in Fig. 8(a) the segmentation obtained with four initial regions $(N = 4)$, and with $\alpha = 0$. Results obtained *without* the region merging prior do not correspond to a meaningful segmentation.

The second example uses the Road image sequence [Fig. 9(a)], which contains two regions: a moving vehicle and a background. The same initialization as with the Marmor sequence was used. Fig. 9 shows the results obtained (using the region merging prior). In Fig. 9(b), one curve remains which separates the moving object from the background; Fig. 9(c) and (d) displays segmentation regions.

We evaluated the interval of α values, $[\alpha_{\min}, \alpha_{\max}]$, which gave the desired number of regions for each sequence. The obtained intervals are reported in Table V. All α values segmenting correctly the Marmor sequence give also the desired number of regions for the Road sequence.

VI. Conclusion

This study investigated a curve evolution method which allowed the effective number of regions to vary during optimization. This was done via a *region merging prior* which, added to a data term and a regularization prior, embeds an implicit region merging in curve evolution, and consequently optimizes the segmentation functional with respect to the number of regions. We gave a statistical interpretation of the weight of this prior. We confirmed this interpretation by several experiments which demonstrated that we can determine automatically, or by learning, an interval of values of this weight applicable to the images of a given class. The method is validated by testing with real images of intensity, color, and motion.

TABLE V
Motion Segmentation: Intervals of α Values Corresponding to the Desired Number of Regions

Sequence	α_{min}	α_{max}
Marmor	1.217	2.69
Camion	0.017	6.5

References

[1] C. Samson, L. Blanc-Féraud, G. Aubert, and J. Zerubia, "A level set model for image classification," *Int. J. Comput. Vis*, vol. 40, no. 3, pp. 187–197, 2000.

[2] P. Martin, P. Réfrégier, F. Goudail, and F. Guérault, "Influence of the noise model on level set active contour segmentation," *IEEE Trans. Pattern Anal. Mach. Intell.*, vol. 26, no. 6, pp. 799–803, Jun. 2004.

[3] M. Rousson and R. Deriche, "A variational framework for active and adaptive segmentation of vector valued images," in *Proc. IEEE Workshop Motion and Video Computing*, Orlando, FL, Dec. 2002, pp. 56–61.

[4] T. F. Chan and L. A. Vese, "Active contours without edges," *IEEE Trans. Image Process.*, vol. 10, no. 2, pp. 266–277, Feb. 2001.

[5] T. F. Chan, B. Y. Sandberg, and L. A. Vese, "Active contours without edges for vector-valued images," *J. Vis. Commun. Image Represent.*, vol. 11, no. 2, pp. 130–141, 2000.

[6] L. A. Vese and T. F. Chan, "A multiphase level set framework for image segmentation using the Mumford and Shah model," *Int. J. Comput. Vis.*, vol. 50, no. 3, pp. 271–293, 2002.

[7] D. Mumford and J. Shah, "Optimal approximation by piecewise smooth functions and associated variational problems," *Commun. Pure Appl. Math*, vol. 42, pp. 577–685, 1989.

[8] S. C. Zhu and A. Yuille, "Region competition: Unifying snakes, region growing, and Bayes/MDL for multiband image segmentation," *IEEE Trans. Pattern Anal. Mach. Intell.*, vol. 18, no. 9, pp. 884–900, Sep. 1996.

[9] D. Cremers, M. Rousson, and R. Deriche, "A review of statistical approaches to level set segmentation: Integrating color, texture, motion and shape," *Int. l J. Comput. Vis.*, vol. 62, no. 3, pp. 249–265, 2007.

[10] A. Yezzi, A. Tsai, and A. Willsky, "A fully global approach to image segmentation via coupled curve evolution equations," *J. Vis. Commun. Image Represent.*, vol. 13, pp. 195–216, 2002.

[11] H. K. Zhao, T. F. Chan, B. Merriman, and S. Osher, "A variational level set approach to multi-phase motion," *J. Comput. Phys.*, vol. 127, pp. 179–195, 1996.
[12] V. Caselles, R. Kimmel, and G. Sapiro, "Geodesic active contours," *Int. J. Comput. Vis.*, vol. 22, pp. 61–79, 1997.
[13] D. Cremers, "Dynamical statistical shape priors for level set based tracking," *IEEE Trans. Pattern Anal. Mach. Intell.*, vol. 28, no. 8, pp. 1262–1273, Aug. 2006.
[14] C. Vazquez, A. Mitiche, and R. Laganiere, "Joint multiregion segmentation and parametric estimation of image motion by basis function representation and level set evolution," *IEEE Trans. Pattern Anal. Mach. Intell.*, vol. 28, no. 5, pp. 782–793, May 2006.
[15] A. Mitiche and H. Sekkati, "Optical flow 3D segmentation and interpretation: A variational method with active curve evolution and level sets," *IEEE Trans. Pattern Anal. Mach. Intell.*, vol. 28, no. 11, pp. 1818–1829, Nov. 2006.
[16] C. Vazquez, A. Mitiche, and I. B. Ayed, "Image segmentation as regularized clustering: A fully global curve evolution method," in *Proc. IEEE International Conf. Image Processing*, Oct. 2004, pp. 3464–3470.
[17] A.-R. Mansouri, A. Mitiche, and C. Vazquez, "Multiregion competition: A level set extension of region competition to multiple region image partitioning," *Comput. Vis. Image Understand.*, vol. 101, no. 3, pp. 137–150, 2006.
[18] I. B. Ayed, N. Hennane, and A. Mitiche, "Unsupervised variational image segmentation/classification using a Weibull observation model," *IEEE Trans. Image Process.*, vol. 15, no. 11, pp. 3431–3439, Nov. 2006.
[19] I. B. Ayed, A. Mitiche, and Z. Belhadj, "Polarimetric image segmentation via maximum likelihood approximation and efficient multiphase level sets," *IEEE Trans. Pattern Anal. Mach. Intell.*, vol. 28, no. 9, pp. 1493–1500, Sep. 2006.
[20] I. B. Ayed and A. Mitiche, "A partition constrained minimization scheme for efficient multiphase level set image segmentation," in *Proc. IEEE Int. Conf. Image Processing*, 2006, pp. 1641–1644.
[21] I. B. Ayed, A. Mitiche, and Z. Belhadj, "Multiregion level set partitioning on synthetic aperture radar images," *IEEE Trans. Pattern Anal. Mach. Intell.*, vol. 27, no. 5, pp. 793–800, May 2005.
[22] T. Kadir and M. Brady, "Unsupervised non-parametric region segmentation using level sets," in *Proc. Int. Conf. Computer Vision*, 2003, pp. 1267–1274.
[23] T. Brox and J. Weickert, "Level set segmentation with multiple regions," *IEEE Trans. Image Process.*, vol. 15, no. 10, pp. 3213–3218, Oct. 2006.
[24] T. Brox and J. Weickert, "Level set based segmentation of multiple objects," in *Proc. DAG*, 2004, vol. 3175, pp. 415–423, LNCS, Springer.
[25] J. M. Geusebroek, G. J. Burghouts, and A. W. M. Smeulders, "The Amsterdam library of object images," *Int. J. Comput. Vis.*, vol. 61, no. 1, pp. 103–122, 2005.
[26] R. O. Duda, P. E. Hart, and D. G. Stork, *Pattern Classification*, 2nd ed. New York: Wiley, 2000.
[27] J. Sethian, *Level Set Methods and Fast Marching Methods*. Cambridge, U.K.: Cambridge Univ. Press, 1999.
[28] R. Nock and F. Nielsen, "Statistical region merging," *IEEE Trans. Pattern Anal. Mach. Intell.*, vol. 26, no. 11, pp. 1452–1458, Nov. 2004.
[29] F. Nielsen and R. Nock, "On region merging: The statistical soundness of fast sorting, with applications," *Comput. Vis. Pattern Recognit.*, pp. 19–26, 2003.

Ismail Ben Ayed (M'04) received the Ph.D. degree in computer science from the Institut National de la Recherche Scientifique, Montreal, Quebec, QC, Canada.

His research is in computer vision, pattern recognition, and medical image analysis. He is currently a Scientist with GE Healthcare, London, ON, Canada.

Amar Mitiche (M'03) received the Licence Ès Sciences degree in mathematics from the University of Algiers, Algeria, and the Ph.D. degree in computer science from the University of Texas at Austin.

He is currently a Professor at the Institut National de Recherche Scientifique (INRS), Department of Telecommunications, Montreal, QC, Canada. His research is in computer vision. His current interests include image segmentation, motion analysis in monocular and stereoscopic image sequences (detection, estimation, segmentation, tracking, 3-D interpretation) with a focus on level set methods, and written text recognition with a focus on neural networks methods.